

# The calculation of the time required to mix liquid metal in a ladle by gas rinsing

by L. W. HELLE\*

## SYNOPSIS

In this investigation, which was conducted at the Metallurgical Research Plant, Lulea, Sweden, a series of experiments were carried out using a water-model to simulate the gas rinsing of a ladle containing liquid metal. The factors examined include the effect of gas flowrate, the position of a porous plug or lance, the immersion depth of the lance, and the geometry of the bath at the time of complete mixing. Mixing times were recorded by conductivity measurements.

The results showed that there is a threshold level for mixing above which no advantage is to be gained from an increase in the gas flowrate. It is suggested that the results can be applied to rinsing ladles in working situations, the levels being approximately 270 dm<sup>3</sup>/min for 40 t ladles and 780 dm<sup>3</sup>/min for 150 t heats.

The optimum siting of the lance or porous plug is a position that is three-quarters of the internal radius from the centre of the ladle with the lance penetrating as deeply as possible into the ladle. The best design of liquid bath is that having a diameter-to-height ratio of 1.

An equation was developed for the calculation, by dimensional analysis, of the time required for mixing during gas rinsing, and a comparison of the calculated mixing times with the results from production trials shows a satisfactory agreement (with a correlation factor of 0,91). Thus, an equation is available for the calculation of the stirring time needed to completely mix the bath in production situations.

## SAMEVATTING

In hierdie ondersoek wat by die Metallurgiese Navorsingsaanleg, Lulea, Swede, ingestel is, is daar 'n reeks eksperimente uitgevoer met gebruik van 'n watermodel om die gasspoeling van 'n gietpot met vloeibare metaal na te boots. Die faktore wat ondersoek is, sluit in die uitwerking van 'n gasvloeitempo, die posisie van 'n poreuse prop of lans, die indompeldiepte van die lans en die geometrie van die bad wanneer die menging voltooi is. Die mengtye is deur geleivermoëmetings geregistreer.

Die resultate het getoon dat daar 'n drupelwaarde vir die menging is waarbo daar geen voordeel uit 'n verhoging van die gasvloeitempo te trek is nie. Daar word aan die hand gedoen dat die resultate op die spoeling van gietpote in werksomstandighede toegepas kan word teen 'n koers van ongeveer 270 dm<sup>3</sup>/min vir 40t-gietpote en 780 dm<sup>3</sup>/min vir 150t-smeltings.

Die optimale plasing van die lans of poreuse prop is 'n posisie wat driekwart van die binneradius vanaf die middelpunt van die gietpot is, terwyl die lans so diep moontlik in die gietpot indring. Die beste ontwerp vir 'n vloeistofbad is een waarin die verhouding van die diameter tot die hoogte 1 is.

Daar is 'n vergelyking vir die berekening van die tyd wat vir menging tydens gasspoeling nodig is op grond van afmetingsontledings ontwikkel en 'n vergelyking van die berekende mengtye met die resultate van die produksieproewe toon 'n bevredigende ooreenkoms (met 'n korrelasiefaktor van 0,91). Daar is dus 'n vergelyking beskikbaar vir die berekening van die roertye wat nodig is om die bad in produksiesituasies volledig te meng.

## Introduction

During the past decade, interest in ladle metallurgy has grown considerably, and the philosophy of steel-making has undergone several changes.

It is now thought that steelmaking should consist of two stages that are carried out in different vessels: the first stage or production of raw steel in a furnace, and the second stage or refining in a ladle. One of the prerequisites for successful ladle treatment is effective mixing of the whole melt. A system of gas rinsing is generally employed to achieve this, the gases, normally argon or nitrogen, being introduced into the melt through porous plugs or a lance.

Opportunities for studying the effectiveness of mixing on a production scale are limited. Equipment is not yet available for continuous measurement, and, in order to obtain formulae that are generally valid, one would have to vary too many parameters. From the economic and practical points of view, this is thought to be difficult or impossible.

Against this background, it is meaningful to study the mixing phenomenon with the help of a simulation technique involving a water-model.

In the investigation described here, this technique was used to show the effect of different parameters on

mixing in a ladle so that ways of minimizing the treatment time could be determined. Simultaneously, an attempt was made to develop an equation from which the required mixing time can be calculated from known data.

## List of Symbols

$a$	surface area of dispersed bubbles	m <sup>2</sup>
$a$	constant, Equation (2)	
$b$	constant, Equation (2)	
$C_p$	heat capacity	J/kg°C
$c$	constant, Equation (7)	
$d$	diameter	m
$F$	function	
$f$	function	
$G$	mass	t
$g$	gravitation constant	m/s <sup>2</sup>
$h$	height of the liquid	m
$M$	molecular mass	g
$p$	pressure	Pa
$R$	gas constant	J/kmol K
$T$	temperature	K
$\dot{V}$	gas flowrate	dm <sup>3</sup> /min
$V$	volume	m <sup>3</sup>
$\gamma$	density (in dimensional analysis)	Ns <sup>2</sup> /m <sup>4</sup>
$\epsilon$	ingoing power	W/ton
$\eta$	dynamic viscosity	Ns/m <sup>2</sup>
$\nu$	cinematic viscosity	m <sup>2</sup> /s
$\zeta$	density	kg/m <sup>3</sup>

\* South African Iron and Steel Industrial Corporation Ltd., P.O. Box 2, Newcastle 2940, Natal.  
© 1981.

$\sigma$	surface tension	N/m
$\tau$	mixing time	s
<i>Indices</i>		
L	liquid	
o	nozzle	

### Experimental

A working unit was simulated in a Plexiglass water-model that was geometrically similar to a 7 t ladle. The model had a diameter of 1000 mm and a height of 1500 mm. Holes were drilled in several positions through the bottom of the model to simulate the effect of porous plugs in different positions on the bottom of a ladle.

The model was fastened to a stand that had the necessary attachments for a lance. The position and immersion depth of the lance could be varied so that it covered the whole volume of the model.

In the tests, measurements were made of the time needed for the conductivity of the water to change after a salt solution had been added. The effect of increasing gas flowrates on mixing time was studied with different combinations of lance or nozzle positions, diameter-to-height ratios, and lance immersion depths. Manometers and rotameters were used to control the gas flow between 50 and 1250 dm<sup>3</sup>/min. The conductivity change was measured by a conductivity meter equipped with a plotter, the necessary probe being situated on the bottom of the model.

The liquid used for the tests was tap water at a temperature of 281 K. The salt solution added was 3M potassium chloride.

Because of the statistical nature of the mixing time, each test was repeated ten times and the average was recorded as the test result.

The production-scale trials were carried out in 40 t and 60 t ladles, and the pilot-plant trials in a 7 t ladle.

The trials proceeded as follows. During gas rinsing, a tracer element was immersed with a pole into the melt, copper, tin, or radioactive gold normally being used. Samples were taken continuously from the melt with sample moulds. It was found that an operator could take 4 to 5 samples per minute, and the sampling continued for about 3 to 6 minutes.

The samples were analysed, and mixing curves were drawn as a function of the variation in concentration of the tracer element.

The mixing time, which was read from the curves, was regarded as the time from the average of the time when the pole was immersed and withdrawn to the time when the melt was completely mixed, i.e. when the variation in concentration read from the mixing curves was less than 5 per cent.

### Results

The mixing phenomena in the model were registered with a plotter, and a typical mixing curve is shown in Fig. 1. The bulk of the solution was considered to be mixed when the variation in conductivity was less than 5 per cent.

#### Calculation of Energy Input

The bulk of the solution is mixed as a result of the power that the ingoing gas delivers into the melt. If

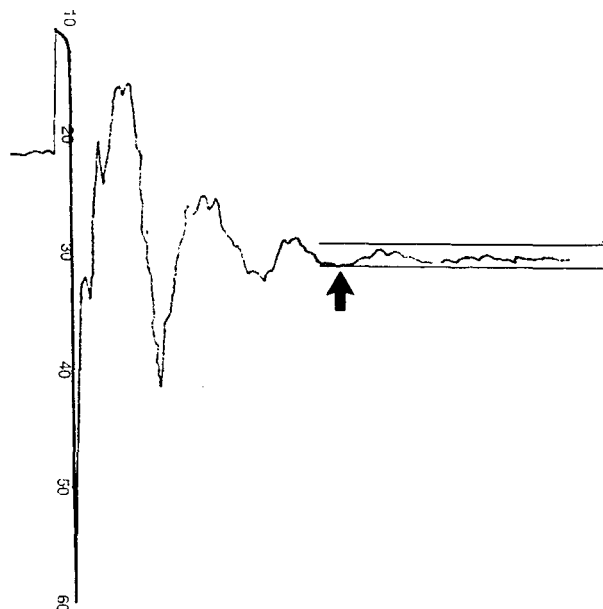


Fig. 1—A typical mixing curve in the water-model tests. The arrow indicates the moment when the bulk of the solution was mixed, i.e. when the variation in conductivity was less than 5 per cent. The speed of the plotter paper was 120 mm/min.

different systems are to be compared, this power has to be calculated when, for example, the temperature, gas flowrate, and mass of the bulk differ from one system to another.

The following equation was developed in the course of this study, the development being detailed in Addendum 1:

$$\dot{c} = 0,014 \frac{\dot{V}T}{G_L} \log\left(1 + \frac{\xi gh}{p_3}\right), \quad (1)$$

where  $\frac{\xi gh}{p_3}$  is  $\frac{h}{10,00}$  for water and  $\frac{h}{1,48}$  for steel

This equation is roughly similar to that developed earlier by Nakanishi *et al.*<sup>1</sup>, using a different method.

#### Effect of Gas Flowrate

When the gas flowrate was varied between 50 and 1250 dm<sup>3</sup>/min, the mixing time decreased as a function of the flowrate. A typical example is shown in Fig. 2. It is noteworthy that the mixing time decreases steeply in the beginning but then levels off. Corresponding results have been reported by Lehrer<sup>2</sup>.

The test programme is given in Table I.

In Table II the results are represented as a function of the power input:

$$\tau = a \dot{c}^b \quad (2)$$

A good average value of the power  $b$  is  $-0,25$ , and this value is used in the calculations given later. Constant  $a$  has to be altered for each test to prevent the mixing curve from becoming steeper or less steep. As a reference point,  $\dot{V} = 200$  dm<sup>3</sup>/min was used. The new values of  $a$  are given in Table II as  $\dot{a}$ .

#### Effect of the Positioning of the Porous Plug and the Immersion Depth of the Lance

Three different positions of the porous plug were

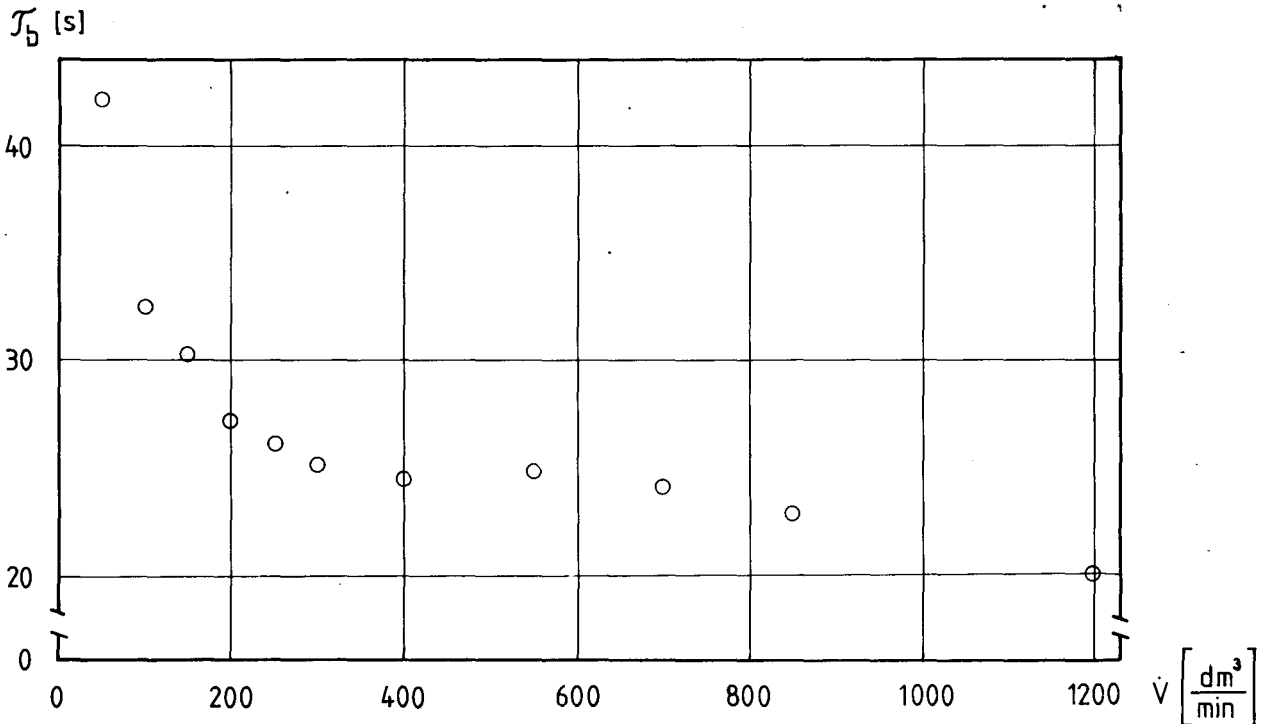


Fig. 2—An example of mixing time decreasing as a function of gas flowrate ( $h = 1\text{m}$ , nozzle position =  $\frac{3}{4}$  radius) — experiment no. 12 of Table I

TABLE I  
TEST PROGRAMME FOR WATER-MODEL EXPERIMENTS

Experiment no.	L m	Nozzle position	$d_0$ mm	$V$ dm <sup>3</sup> /min
1	0,25	○	15,7	50-1200
2		3/4	15,7	50-1200
3		⋮	8,0	50-1200
4	0,70	○	15,7	50-1200
5		3/4	15,7	50-1200
6		⋮	8,0	50-1200
7	1,0	○	8,0	50-1200
8		3/4	8,0	50-1200
13		⋮	8,0	50-1200
9		○	11,7	50-1200
10		3/4	11,7	50-1200
11		⋮	15,6	50-1200
12		3/4	15,6	50-1200
14	1,3	○	20,8	50-1200
15		3/4	20,8	50-1200
16		⋮	15,7	50-1200
17	1,0	○	15,7	50-1200
18		3/4	15,7	50-1200
19		⋮	8,0	50-1200
20	1,0	L <sub>90</sub> ○	20,8	50-1200
21		L <sub>90</sub> 3/4	20,8	50-1200
22		L <sub>30</sub> ○	20,8	50-1200
22		L <sub>30</sub> 3/4	20,8	50-1200

○ = nozzle positioned in the centre, 3/4 = nozzle positioned at three-quarters the radius, ⋮ = three nozzles in a profile of an equilateral triangle, each at three-quarters the radius, L<sub>90</sub> = lance immersion 90%, L<sub>30</sub> = lance immersion 30%.

examined, i.e. gas was blown to the model through nozzles in different positions on the bottom of the model.

The shortest mixing time was achieved by the use of three nozzles positioned in a profile of an equilateral triangle, each nozzle at a distance of one-quarter the

radius from the wall. The second shortest mixing time was achieved with one nozzle positioned at three-quarters the radius of the ladle bottom, and the longest mixing time of the three positions examined was obtained with a nozzle positioned at the centre of the ladle bottom. The same tendency is valid for a lance.

As can be expected, the immersion depth of the lance influences the mixing time greatly, i.e. the deeper the immersion, the shorter the mixing time.

TABLE II  
THE RESULTS FROM THE WATER-MODEL TESTS IN THE FORM OF MIXING TIME AS A FUNCTION OF INGOING POWER,  $\tau = a\epsilon^b$ .

Experiment no.	$a$	$b$	$a'$
1	128,2978	-0,2258	140,562
2	107,8059	-0,2101	125,200
3	124,1300	-0,2538	122,383
4	89,3517	-0,2289	96,665
5	87,5672	-0,2477	88,365
6	58,6334	-0,1926	72,757
7	86,3921	-0,2517	85,782
8	90,8206	-0,2694	84,513
9	79,2598	-0,2212	88,320
10	82,3927	-0,2317	88,320
11	64,8172	-0,1882	81,720
12	62,4088	-0,2093	72,585
13	69,8421	-0,2482	70,301
14	108,2539	-0,3066	87,813
15	111,8113	-0,3175	87,051
16	96,9778	-0,2735	88,765
17	83,7738	-0,2668	78,650
18	80,6008	-0,2699	74,856
19	106,8396	-0,2616	102,279
20	99,1099	-0,2825	87,813
21	272,7384	-0,2771	246,434
22	487,6238	-0,4694	215,417

The numbers indicate the respective numbers in Table I,  $a'$  is  $a$  corrected as explained in the text

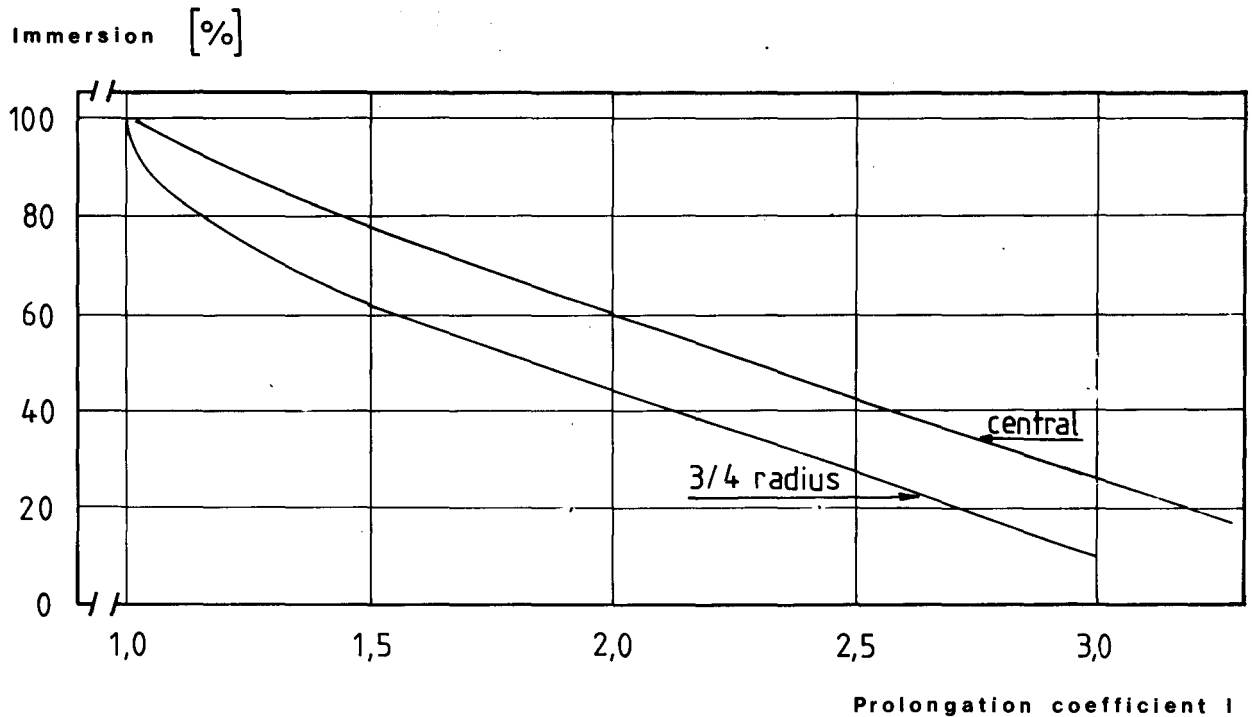


Fig. 3—Prolongation coefficient of mixing when a lance is used to introduce the rinsing gas into the melt

Fig. 3 represents the prolongation coefficient of mixing as a function of the percentage of the immersion depth of the lance at different depths in a standard melt.

The prolongation coefficient indicates the degree to which the mixing time will be extended for a certain depth of immersion and position of the lance compared with a standard mixing time when the liquid is bubbled through a porous plug in the same position as the lance on the ladle floor.

#### Effect of Geometry

One might assume that, when the volume of liquid decreases, i.e. when the height decreases but the diameter remains the same, mixing time becomes shorter. However, this was not the case. As can be seen from Fig. 4, the mixing time as a function of the  $d/h$  ratio (diameter to height) takes on a V-shape. All the test results followed the same pattern.

The minimum mixing time was achieved when the  $d/h$  was 1. When the  $d/h$  either decreased or increased, the mixing time became longer.

#### Effect of Surface Tension

Szekely<sup>3</sup> gives a relationship between the surface area of the dispersed bubbles and the surface tension proportionally:

$$a \approx \sigma^{-3} \quad (3)$$

Equation (3) shows that the surface area decreases when the surface tension increases, i.e. the bubbles become bigger, and, when the surface tension decreases, the size of the bubbles also decreases.

In the water-model, the effect of surface tension was investigated by decreasing it with the addition of propyl alcohol (0,4 per cent of the volume of the water). Table III summarizes the effect of the surface tension on the mixing time and on the size and amount of bubbles.

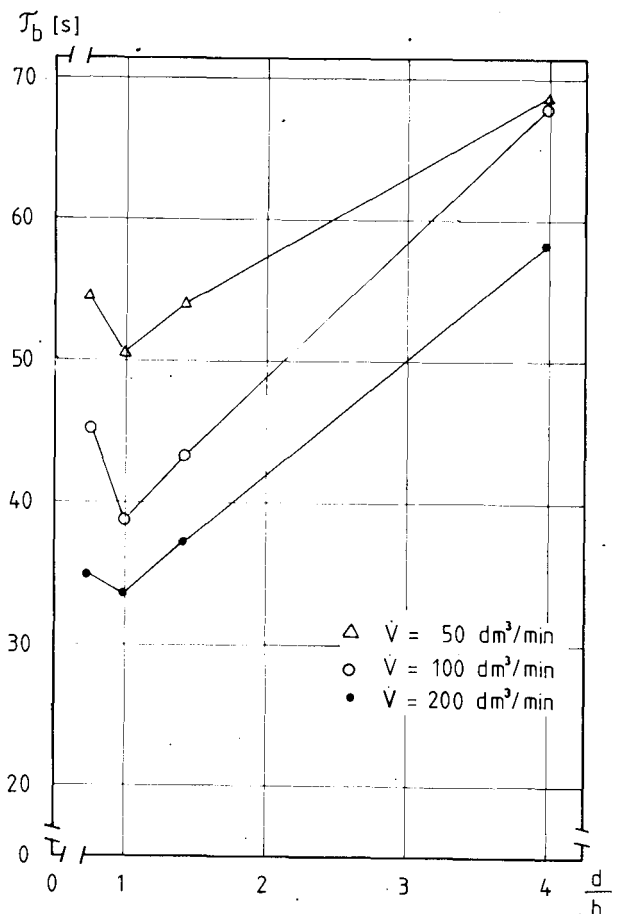


Fig. 4—Mixing time as a function of diameter-to-height ratio (nozzle positioned at the centre of the bottom)

TABLE III

MIXING TIME, AND SIZE AND AMOUNT OF BUBBLES, VERSUS SURFACE TENSION

Liquid	H <sub>2</sub> O + C <sub>3</sub> H <sub>7</sub> OH	H <sub>2</sub> O(25°C)	Steel
τ, s (V = 50 dm <sup>3</sup> /min)	43,2	50,2	
σ, N/m	0,05908	0,07197	1,350
a, equation (3)	2,57	2,40	0,90
Amount of bubbles	Big	Less	Small
Size of bubbles	Small	Bigger	Big

The quantity of bubbles in the different mixtures was assessed visually. The quantity of bubbles in steel was deduced from these assessments. The size of the bubbles in the propanol mixture and in water was about 1 mm and 3 mm respectively (visual assessment). The size of the bubbles in steel was assumed to be greater than that of the bubbles in the aqueous media owing to the higher surface tension.

The conclusions that can be drawn from this are that a lower surface tension means a larger amount of small bubbles and a shorter mixing time, and a higher surface tension means less but larger bubbles and a longer mixing time.

Effect of Other Parameters

When the diameter of the nozzle was varied between 8,0 and 20,8 mm, no clear effect on the mixing time was apparent. Therefore, it appears that the effect of the nozzle size on the field covered in this study is negligible.

The dynamic viscosity was increased by changing the temperature of the water. The viscosity of water is 0,001 Ns/m<sup>2</sup> at 20°C and 0,0014 Ns/m<sup>2</sup> at 8°C. The results showed that a higher viscosity meant a longer mixing time, as can be expected. However, the difference is relatively small, only 6 per cent. Similar results were reported by Shevtsov<sup>4</sup>. According to his findings, an increase of 250 per cent in viscosity caused a 17 per cent increase in mixing time.

Results of the Dimensional Analysis

The definition of the relevant parameters is the Achilles' heel of the whole dimensional analysis. All the parameters that affect the system have to be included, but only once. This means that, if one parameter is considered to be a function of some others, it should be excluded.

The following parameters were chosen to represent the system:

$$\tau, \gamma, \epsilon, \eta, h, d, \sigma \dots \dots \dots (4)$$

Various methods of dimensional analysis are available. The best-known methods are apparently the Buckingham Pi theorem and Rayleigh's method. However, a method not so well known but more serviceable, developed by Salin<sup>5</sup>, was used in this study.

According to the analysis, described in detail in Addendum 2, the system depends on four dimensionless groups as follows:

$$\frac{\tau\eta}{h^2\gamma} = F\left(\frac{h^4\gamma^3\epsilon}{\eta^3}; \frac{h\sigma\gamma}{\eta^2}; \frac{d}{h}\right) \dots \dots \dots (5)$$

If τ is a power function of three dimensionless groups, the average power for ε being -0,25,

$$\tau = f\left[\frac{h^2\gamma}{\eta}\left(\frac{h^4\gamma^3}{\eta^3}\epsilon\right)^{-0,25}; \frac{h\sigma\gamma}{\eta^2}; \frac{d}{h}\right], \dots \dots (6)$$

and further, in power form,

$$\tau = k\left(\frac{d}{h}\right)^b \left(\frac{h\sigma\gamma}{\eta^2}\right)^c (h\nu^{-0,25}) \epsilon^{-0,25} \dots \dots (7)$$

The next step is the calculation of the constants k, b, and c.

Constant c

If V̇, T, G<sub>L</sub>, d, h, γ, and η are the same in two different cases (H<sub>2</sub>O + C<sub>3</sub>H<sub>7</sub>OH and H<sub>2</sub>O at 25°C), equation (7) differs only by the term that includes surface tension. Therefore, one can write

$$\frac{\tau_1}{\tau_2} = \frac{\left(\frac{h\sigma\gamma}{\eta^2}\right)_1^c}{\left(\frac{h\sigma\gamma}{\eta^2}\right)_2^c}, \dots \dots \dots (8)$$

in which index 1 refers to H<sub>2</sub>O at 25°C and index 2 to H<sub>2</sub>O + C<sub>3</sub>H<sub>7</sub>OH.

By substituting from Table III, taking logarithms, and re-arranging one gets c = 0,3.

Constants k and b

The calculation of k and b is carried out as a function of the position of the nozzle on the bottom of the model. The principle of the solution is represented with the help of an example in Addendum 3. The results are as follows:

- for the nozzle positioned in the middle of the bottom, k = 0,0163 and b = 1,617,
- for the nozzle positioned at three-quarters the radius, k = 0,0145 and b = 1,619,
- for three nozzles positioned in a profile of an equilateral triangle, k = 0,0134 and b = 1,634.

Discussion

Fig. 2 shows mixing time versus gas flowrate. Only up to about 310 dm<sup>3</sup>/min (65 W/t according to equation (1) in this particular case) does the mixing time decrease, but above this value it remains relatively stable. Thus, it appears that the use of rinsing gas in excess of 65 W/t is wasteful. This amount is roughly equal to 270 dm<sup>3</sup>/min on a scale of 40 t and 780 dm<sup>3</sup>/min on a scale of 150 t calculated according to equation (1) on the assumption that the bath heights are 2 and 2,9 m respectively.

This calculation is based on a geometry similar to that of the model (d/h = 1) with the porous plug positioned at three-quarters the radius. However, because of the difference in physical size, the actual mixing time will not be the same even though the power input per ton is the same.

As it appears from the model tests, porous plugs positioned in practical cases at three-quarters the radius are superior to the central position in minimizing the mixing time. Similarly, the deeper the immersion of a lance, the shorter the mixing time. Simultaneously, the deeper immersion of the lance may assist in preventing dead volumes in the lower part of the ladle.

Somewhat surprisingly, the geometry of the liquid volume greatly affects the mixing time. This can be due to the disturbances in the flow pattern when  $d/h$  is far from the value 1. Observations in the model with, for example, a liquid height of 0,25 m ( $d/h = 4$ ) have shown that the necessary continuous flow is completely missing and the liquid is not affected by the bubbling operation.

The validity of equation (7) for the calculation of mixing time can be tested against the results from the production trials. Trial data are given in Table IV and the comparison is represented in Fig. 5.

From Fig. 5 it appears that, because the correlation factor is as good as 0,91, the equation developed can be

used for the calculation of the mixing time with the accuracy demanded in actual production.

The slope of a linear regression curve calculated from the experimental and calculated mixing times in Table IV is 0,94 (ideally 1). This means that equation (7) gives consistently long mixing times. This may be because the effect of thermal convection was not taken into account. On the scale of 40 to 50 t, the circulation of the melt due to convection can reach 15 to 225 t/min<sup>6</sup>, which can give an increase of about 25 per cent to the mixing power and thus make the actual mixing time shorter compared with the calculated value.

### Conclusions

The use of a water-model to simulate gas flow and of conductivity measurement was shown to be a suitable and graphic method of examining the mixing efficiency in metallurgical ladles.

It appears from the results obtained with the model that there is a maximum gas flowrate above which no significant decrease of mixing time can be achieved.

The best position for a porous plug is, as expected, at three-quarters the radius. Even better than this is a system of three porous plugs each at three-quarters the radius, forming the profile of an equilateral triangle. From the point of view of the mixing time, the deepest possible immersion of the lance is best.

A diameter-to-height ratio of the liquid as close to 1 as possible gives an ideal flow pattern in the ladle.

The results show that the equation developed in this study for the calculation of the mixing time required during gas rinsing can be used with sufficient accuracy for production purposes.

### Acknowledgments

This paper arose from a research programme undertaken jointly by the Metallurgical Research Plant, Lulea, Sweden, and Jernkontoret, Stockholm, Sweden. The author thanks the management of the Metallurgical Research Plant for permission to publish this paper. Special thanks are due to Mr T. Lehner for the advice and supervision he gave during the course of the work.

### References

1. NAKANISHI, K., *et al.* Possible relationship between energy dissipation and agitation in steel processing operations. *Ironmaking Steelmaking*, no. 3, 1975. pp. 193-197.
2. LEHRER, L. H. Gas agitation of liquids. *I & EC Process Design and Development*, vol. 7, no. 2. 1968. pp. 226-239.
3. SZEKELY, J. T., *et al.* *Rate phenomena in process metallurgy*. New York, Wiley-Interscience, 1971. 748 pp.
4. SHEVTSOV, E. K., *et al.* The efficiency of mixing of a steel-making bath. *Izv. VUZ, Chern. Met.*, no 7. 1977. pp. 43-45.
5. KUUSINEN, J., *Rationalization of technical calculations and dimensional analysis for model research*. Helsinki, Swedish Academy for Technical Sciences in Finland, *Publication* no. 10. 1936. 53 pp. (In Swedish).
6. VERHOOG, H. M., *et al.* Heat balance and stratification of liquid steel in ladles. *ESTEL Ber.*, no 3. 1974. pp. 114-120.

### Addendum 1

Gas is fed continuously into a system and the process is stationary. Agitation is thus gained from the 'technical' work<sup>1</sup> supplied by the gas (Fig. A1).

TABLE IV

DATA FROM THE PRODUCTION-SCALE EXPERIMENTS. IN THE MEFOS EXPERIMENTS, THE LANCE WAS POSITIONED AT THE CENTRE. IN THE PRODUCTION-SCALE EXPERIMENTS, THE LANCE WAS POSITIONED AT THREE-QUARTERS THE RADIUS EXCEPT THE CASES IN WHICH A POROUS PLUG WAS USED POSITIONED AT THE CENTRE

$V$ dm <sup>3</sup> /min	$T$ K	$G_L$ t	$d$ m	$h$ m	Immer- sion depth %	$\tau$ cal. s	$\tau$ exp. s
650	1 818	6	1	1	80	46	42
100	1 860	5	1	0,85	76	82	78
440	1 853	5	1	0,85	76	56	45
600	1 878	6,7	1	1,1	86	41	30
40	1 809	6,5	1	1,1	86	80	136
40	1 821	6,5	1	1,1	36	166	175
40	1 821	6,5	1	1,1	36	166	177
580	1 873	6	1	0,92	87	43	40
530	1 876	6,7	1	1,03	10	116	101
680	1 908	40	1,86	2,1	55	177	110
620	1 903	40	1,86	2,1	90	88	70
570	1 948	38	1,86	2,0	15	249	180
680	1 908	38	1,86	2,0	85	91	60
570	1 878	38	1,86	2,0	90	91	50
22	1 873	39,5	1,92	2,1	86	222	225
68	1 873	40,9	1,92	1,95	90	168	219
55	1 823	52,7	2,37	1,4	porous plug	343	360
450	1 823	50,1	2,37	1,35	porous plug	204	120

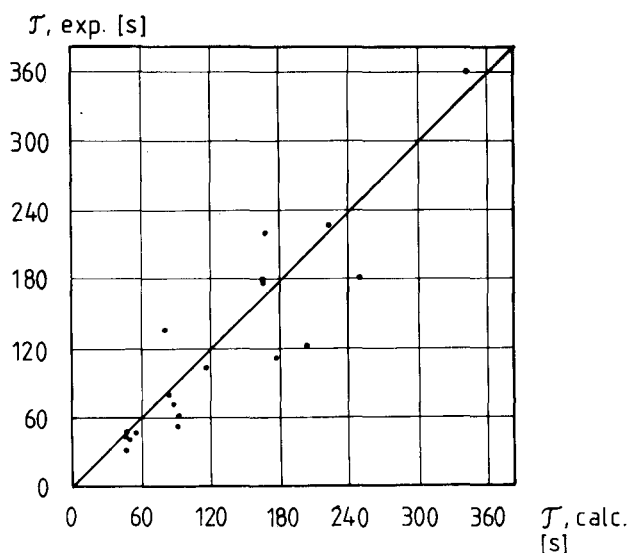
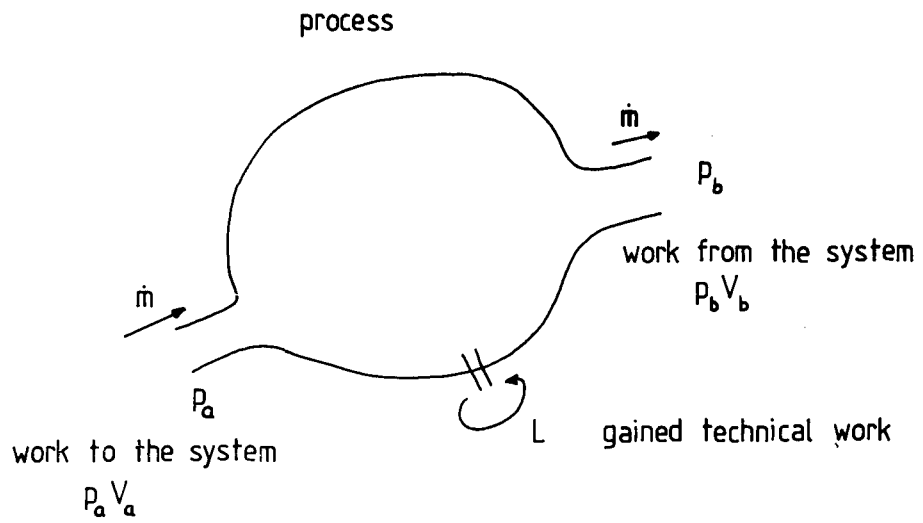
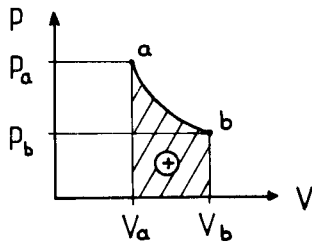


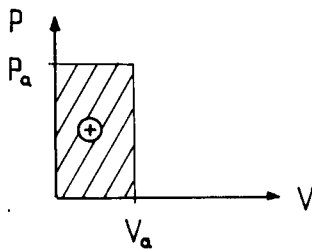
Fig. 5—Comparison of mixing times in production-scale experiments calculated according to equation (7) ( $\tau$  calc.) and obtained experimentally ( $\tau$  exp.):  $\gamma = 7000 \text{ N s}^2/\text{m}^4$ ,  $\eta_L = 0,007 \text{ N s}/\text{m}^2$ ,  $\sigma = 1,35 \text{ N}/\text{m}$ .



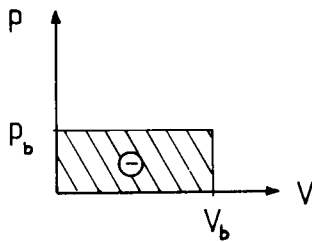
total work from the system  $\int_a^b p dV = -p_a V_a + L + p_b V_b$



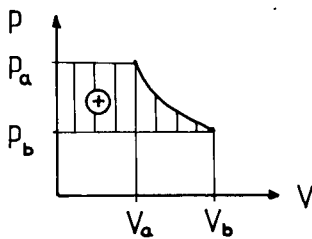
total compression work



compression work, in



compression work, out



gained technical work  $L$

Fig. A1—Technical work from a closed system

The total compression work from the system was divided as follows (Fig. A1):

$$\int_a^b p dV = -p_a V_a + L + p_b V_b, \text{ or}$$

$$L = \int_a^b p dV - \int_a^b -d(pV)$$

$$L = - \int_a^b V dp,$$

Energy equation (1st main principle):

Ingoing heat  $dq$   
 Gained technical work  $dW = -Vdp$   
 Increase of enthalpy  $dH$   
 $dq = dW + dH$

Here it is assumed that the heating up of the ingoing gas takes place extremely quickly, depending on the great difference in temperatures between the melt and the gas. For the sake of calculation, the momentary isobaric heating of the gas up to the temperature of the melt,  $T_2$ , was calculated, and after that an isothermal expansion up to the ambient pressure.

For an ideal gas, the following is valid:

$$pV = R_m T \rightarrow dW = -Vdp = -R_m T \frac{dp}{p} \quad \left| R_m = \frac{R}{M} \right.$$

$$dH = C_p dT$$

But isothermally  $dT = 0 \rightarrow dH = 0$ .

Thus,  $dq = dW$ ;  $dW = -R_m T_2 \frac{dp}{p}$

Gained agitation work:

$$L = \int_1^3 dW = R_m T_2 \ln \frac{p_2}{p_3} \quad \left| p_2, p_3 \text{ see Fig. A2.} \right.$$

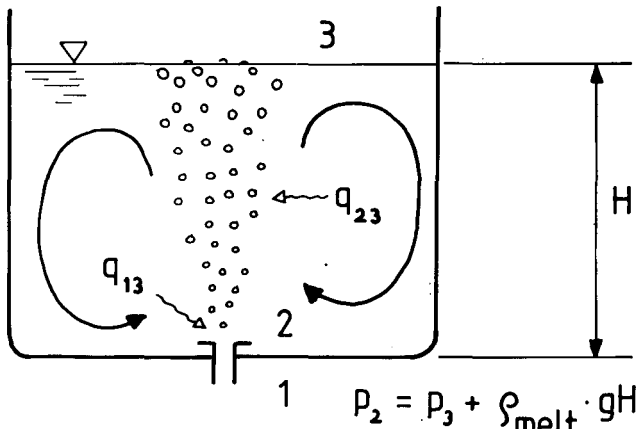


Fig. A2—Pressure in different positions of the system

From a  $p - V$  diagram (Fig. A3), one can see that an increase of the volume 1-2 as a result of the isobaric heating does not give any direct addition to the agitation work

$$\left( \int_1^2 V dp = 0 \right),$$

but, conversely, it gives an addition indirectly by increasing the temperature of the work medium and thereby the outgoing volume  $V_2$  before expansion as well as increasing the expansion work itself.

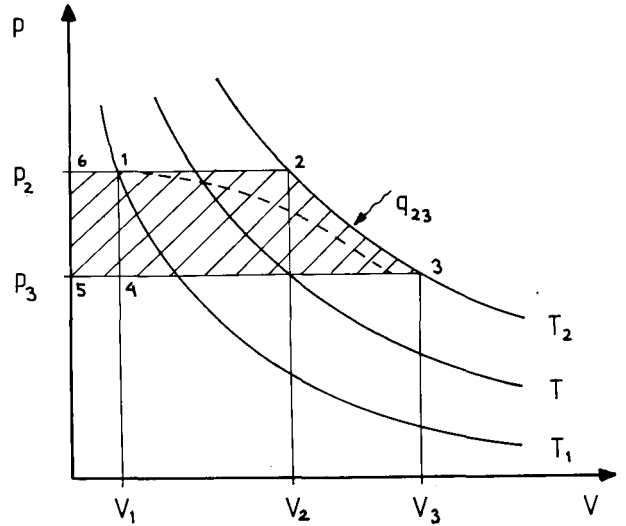


Fig. A3— $p - V$  diagram

Even the work done by buoyancy was included in

$$L = - \int_1^3 V dp,$$

and one finds, for example, that light, incompressible 'balls' pumped into the vessel through its bottom deliver an amount of agitation that can be represented by the area 6-1-4-5 (Fig. A3).

One incompressible 'ball' with density  $\rho$  delivers buoyancy work per mass unit:

$$L = \frac{Fh}{m} = \frac{1}{\xi} \cdot g \cdot (\xi L - \xi) \cdot h$$

$$= \frac{1}{\xi} \underbrace{(gh\xi L)}_{V_1 p_2 - p_3} \underbrace{\left(1 - \frac{\xi}{\xi}\right)}_{\approx 1}$$

$$= V_1 (p_2 - p_3)$$

When the heating up of the gas does not take place immediately, the situation changes according to the dotted line in Fig. A3, and the ideal work decreases.

The agitation gained was thus

$$L = R_m T_2 \ln \frac{p_2}{p_3}$$

$$= R_m T_2 \ln \left( \frac{p_3 + \xi L g h}{p_3} \right)$$

If it is assumed that gas is pumped into the vessel with the velocity  $\dot{V}$  ( $\text{dm}^3/\text{min}$ ) and that the gas flow disperses to bubbles with the amount  $N$ ,

$$NL = R_m T_2 \dot{V} \ln \left( 1 + \frac{\xi L g h}{p_3} \right)$$

and further the ingoing power per ton of liquid or melt,

$$\dot{\epsilon} = 0,014 \frac{\dot{V}T}{G_L} \log \left( 1 + \frac{\xi L s h}{p_3} \right),$$

in the water

$$\frac{\xi g h}{p_3} \text{ is } \frac{h}{10,00}$$

and in the case of steel

$$\frac{h}{1,48}$$

### Reference

1. PERRY, J. H. Chemical engineer's handbook. Tokyo. Mc Graw-Hill, 1963

### Addendum 2

$$\gamma = \frac{Ns^2}{m^4}$$

$$\dot{\epsilon} = \frac{\frac{Nm}{s}}{\frac{Ns^2}{m}} = \frac{m^2}{s^3}$$

$$\eta = \frac{Ns}{m^2}$$

$$\tau = s$$

$$h = m$$

$$d = m$$

$$\sigma = \frac{N}{m}$$

1st step:  $\gamma$  is used as a cancellor

$$\dot{\epsilon} = \frac{m^2}{s^3}$$

$$\frac{1}{\gamma} \eta = \frac{Ns}{m^2} \cdot \frac{m^4}{Ns^2} = \frac{m^2}{s}$$

$$\tau = s$$

$$d = m$$

$$h = m$$

$$\frac{1}{\gamma} \sigma = \frac{N}{m} \cdot \frac{m^4}{Ns^2} = \frac{m^3}{s^2}$$

2nd step:  $\tau$  is used as a cancellor

$$\tau^3 \dot{\epsilon} = \frac{m^2}{s^3} \cdot s^3 = m^2$$

$$\frac{1}{\gamma} \eta = \frac{m^2}{s} \cdot s = m^2$$

$$d = m$$

$$h = m$$

$$\tau^2 \cdot \frac{1}{\gamma} \sigma = \frac{m^3}{s^2} \cdot s^2 = m^3$$

3rd step:  $h$  is used as a cancellor

$$\frac{1}{h^2} \tau^3 \dot{\epsilon} = m^2 \cdot \frac{1}{m^2} = ( )$$

$$\frac{1}{h^2} \tau \frac{1}{\gamma} \eta = m^2 \cdot \frac{1}{m^2} = ( )$$

$$\frac{1}{h} d = m \cdot \frac{1}{m} = ( )$$

$$\frac{1}{h^3} \tau \frac{1}{\gamma} \sigma = m^3 \cdot \frac{1}{m^3} = ( )$$

Thus,

$$\frac{\tau \eta}{h^2 \gamma} = F \left( \frac{\tau^3 \dot{\epsilon}}{h^2} ; \frac{d}{h} \frac{\tau^2 \sigma}{h^3 \gamma} \right).$$

which can be re-arranged

$$\frac{\tau \eta}{h^2 \gamma} = F \left( \frac{\tau^3 \dot{\epsilon}}{h^2} \frac{h^6 \gamma^3}{\tau^3 \eta^3} ; \frac{\tau^2 \sigma}{h^3 \gamma} \frac{h^4 \gamma^2}{\tau^2 \eta^2} ; \frac{d}{h} \right).$$

And finally

$$\frac{\tau \eta}{h^2 \gamma} = F \left( \frac{h^4 \gamma^3}{\eta^3} \dot{\epsilon} ; \frac{h \sigma \gamma}{\eta^2} ; \frac{d}{h} \right)$$

### Addendum 3

With a nozzle diameter of 15,6 mm and the nozzle positioned at the centre, there are two equations:

$$\tau = a' \dot{\epsilon}^b \quad (2)$$

$$\tau = k \left( \frac{d}{h} \right)^b \left( \frac{h \sigma \gamma}{\eta^2} \right)^{0,3} (h \nu^{-0,25}) \dot{\epsilon}^{-0,25} \quad (7)$$

Now

$$a' (2) = k \left( \frac{d}{h} \right)^b \left( \frac{h \sigma \gamma}{\eta^2} \right)^{0,3} (h \nu^{-0,25}) (7)$$

$$\text{or } k \left( \frac{d}{h} \right)^b = \frac{a'}{\left( \frac{h \sigma \gamma}{\eta^2} \right)^{0,3} (h \nu^{-0,25})} = y,$$

which can be solved in the form

$$y = k \left( \frac{d}{h} \right)^b ; \ln y = \ln k + b \ln \frac{d}{h}$$

The answer can be read direct, after the values of  $\ln y$  and

$$\ln \left( \frac{d}{h} \right)$$

from the model results (Tables I and II), have been tabulated as follows:

$h_L$	$\ln \left( \frac{d}{h} \right)$	$\ln y$
1,3	-0,262	-4,459
1	0	-4,200
0,7	0,3567	-3,569
0,25	1,386	-1,856

Similarly, the values of  $k$  and  $b$  can be calculated for a nozzle positioned at three-quarters the radius and for three nozzles in an equilateral triangle.